Electronic Supplementary Material (ESI) for Journal of Materials Chemistry A.
This journal is © The Royal Society of Chemistry 2017

Supplementary Information

Electrocatalytic Reduction of CO_2 to CO with 100% Faradaic Efficiency by Pyrolyzed Zeolitic Imidazolate Frameworks Supported on Carbon Nanotube Networks

Ying Guo,[†a] Huijuan Yang,[†a] Xin Zhou,[ab] Kunlong Liu,[a] Chao Zhang,[a] Zhiyou Zhou,[a] Cheng Wang*[a] and Wenbin Lin[ac]

a. Collaborative Innovation Center of Chemistry for Energy Materials, State Key Laboratory of Physical Chemistry of Solid Surfaces, Department of Chemistry, College of Chemistry and Chemical Engineering, Xiamen University, Xia-men 361005, P.R. China.
b. School of Chemistry and Chemical Engineering, South China University of Technology, Guangzhou 510640, PR China.
c. Department of Chemistry, University of Chicago, 929 E 57th Street, Chicago, IL 60637, USA.

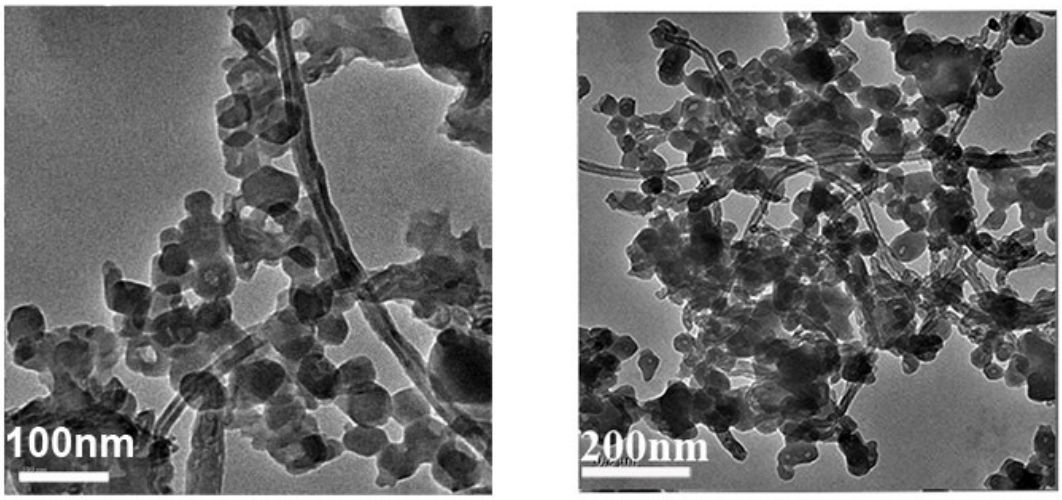

Fig. S1 TEM images of **ZIF-CNT-FA** (a) and **ZIF-Fe-CNT-FA** (b).

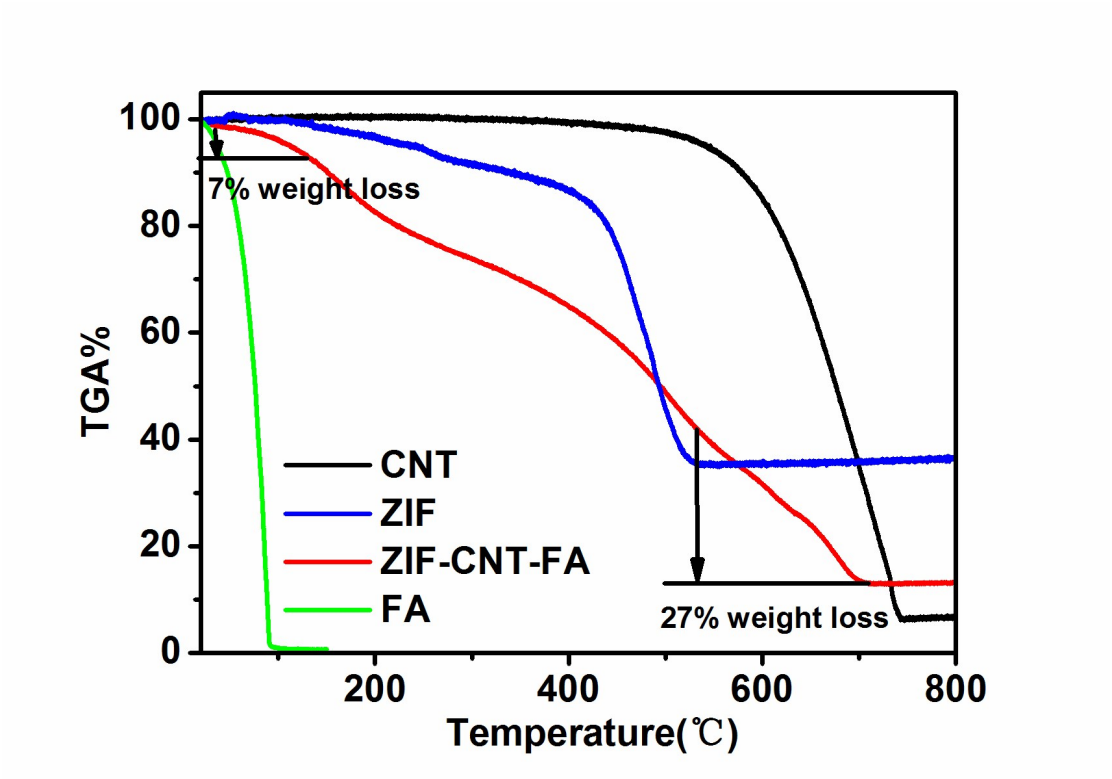

Fig. S2 TGA of CNT, FA, ZIF-8, and **ZIF-CNT-FA** under nitrogen.

We attributed the weight-loss of **ZIF-CNT-FA** in the temperature range between 25 and 130 °C to the thermal decomposition of furfuryl alcohol (FA) and in the temperature range between 530 and 800 °C to the thermal decomposition of CNT.

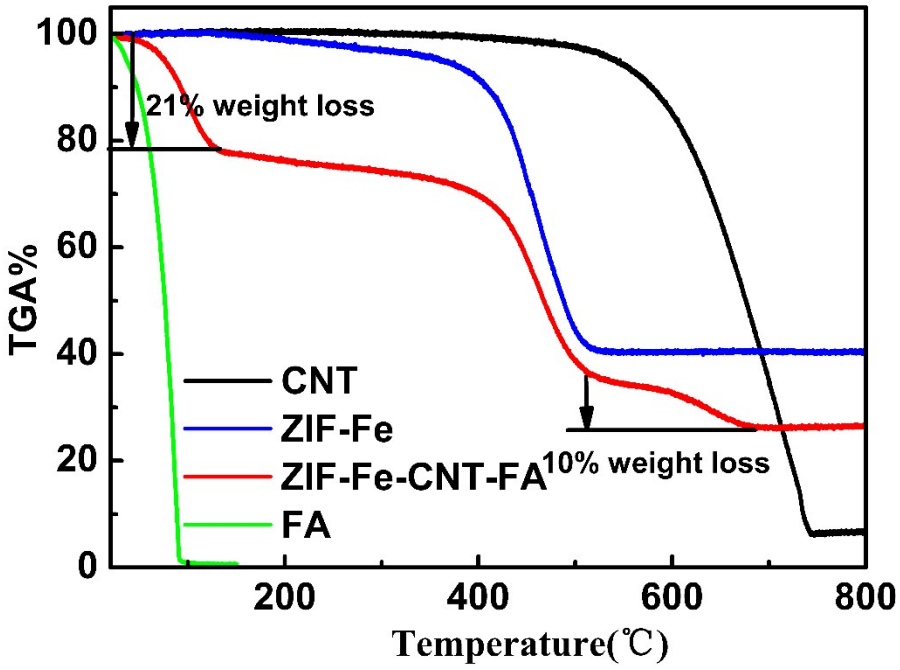

Fig. S3 TGA of CNT, FA, ZIF-Fe, and **ZIF-Fe-CNT-FA** under nitrogen.

We attributed the weight-loss of **ZIF-Fe-CNT-FA** in the temperature range between 25 and 130 °C to the thermal decomposition of furfuryl alcohol (FA) and in the temperature range between 520 and 800 °C to the thermal decomposition of CNT.

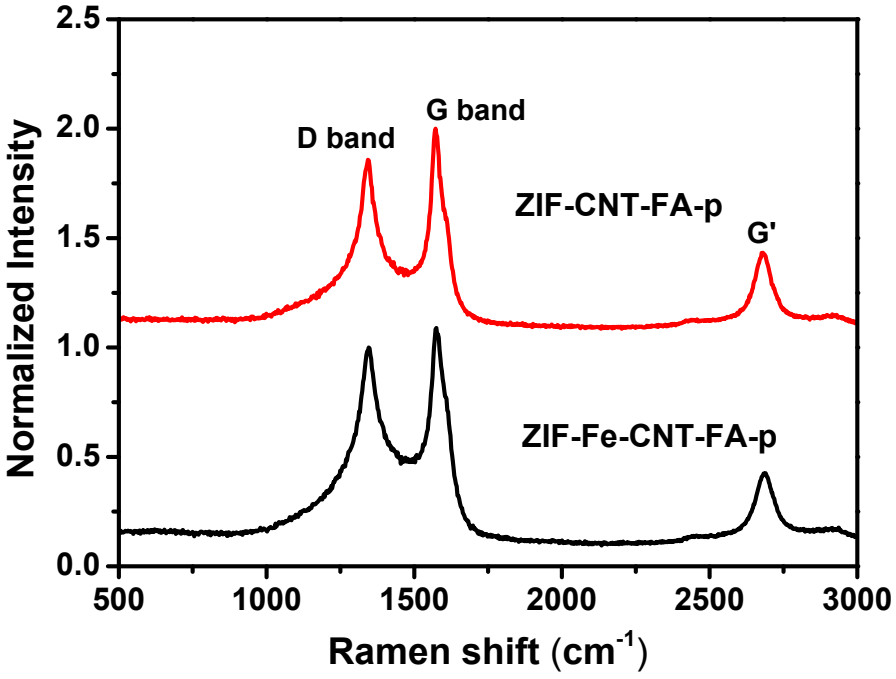

Fig. S4 Raman spectra of pyrolyzed ZIF samples.

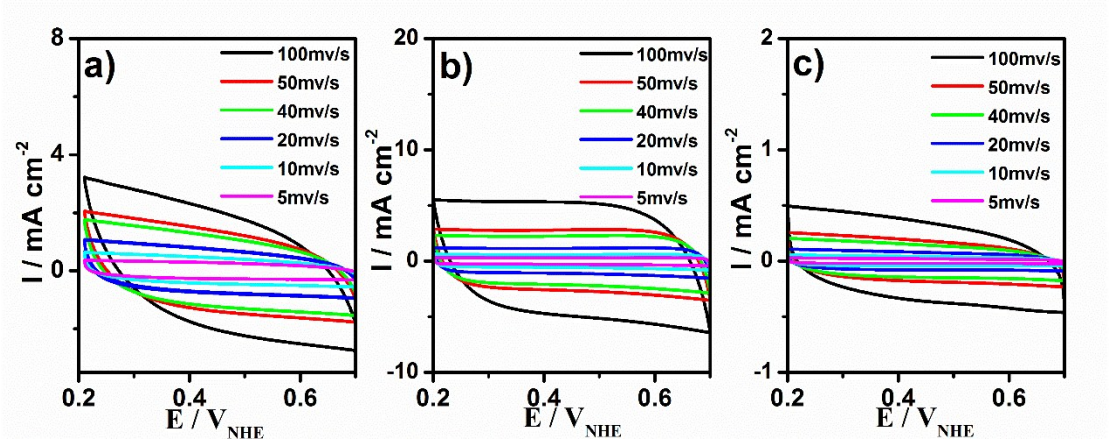

Fig. S5 Cyclic voltammograms of different electrodes studied in 0.1 M Na_2SO_4 (degassed with N_2) at various scan rates for the estimation of double layer capacitances. (a) **ZIF-Fe-CNT-FA-p**, (b) **ZIF-CNT-FA-p**, and (c) **ZIF-FA-p**. The geometric area of all electrodes is 0.07 cm^2 and the loading of catalysts is 0.06 mg.

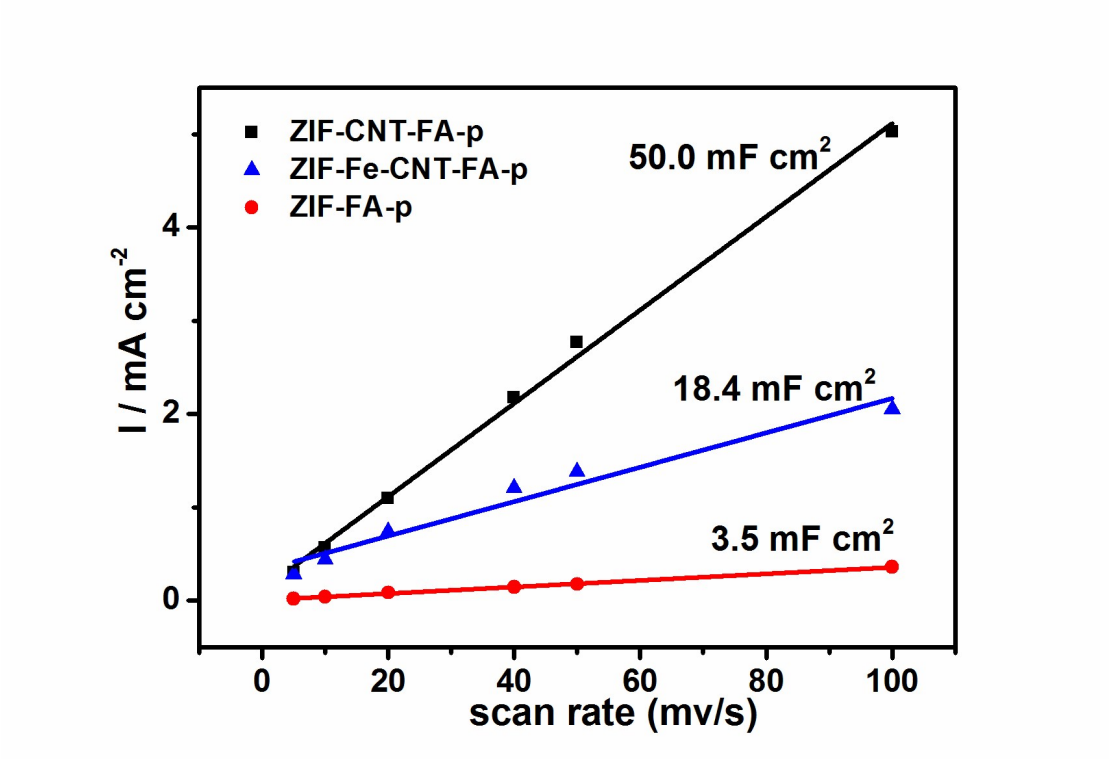

Fig. S6 Double layer capacitances of **ZIF-CNT-FA-p**, **ZIF-Fe-CNT-FA-p**, and **ZIF-FA-p**. The C_{dl} was estimated by plotting the $\Delta j = (ja - jc)$ at 0.45 V_{NHE} (where j_a and j_c are the anodic and cathodic current densities, respectively) against the scan rate, in which the slope was twice that of C_{dl}.

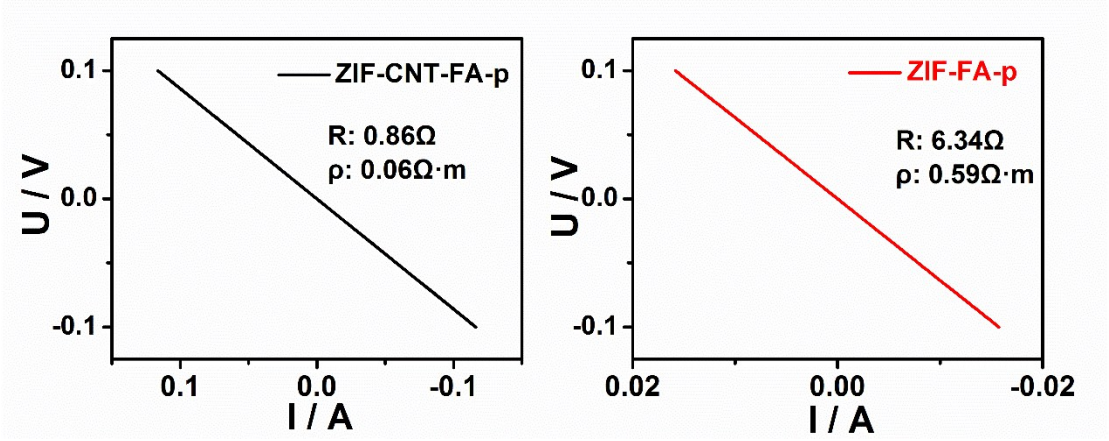

Fig. S7 I–V curves of **ZIF-CNT-FA-p** and **ZIF-FA-p**.

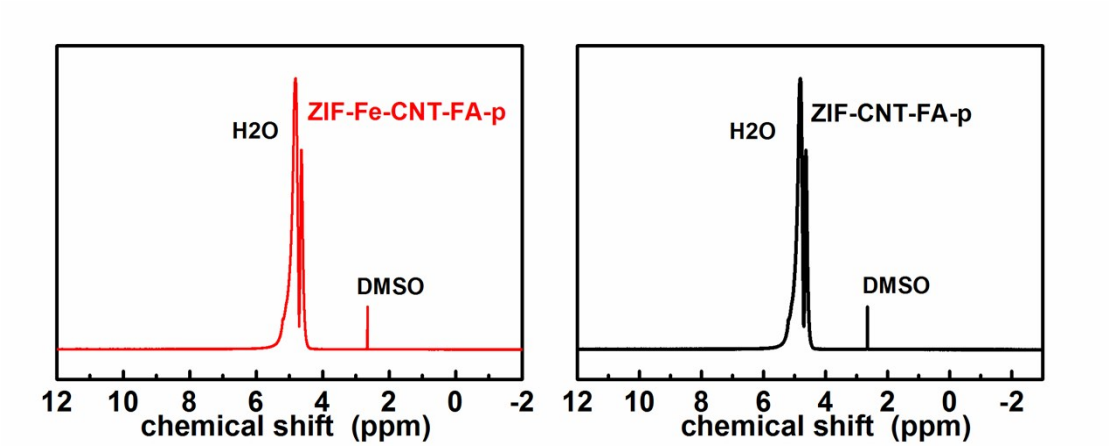

Fig. S8 Representative ^{1}H-NMR spectra of the electrolyte solution after CO_2 reduction electrolysis at -0.86 V_{RHE} for the **ZIF-CNT-FA-p,** and -0.56 V_{RHE} for the **ZIF-Fe-CNT-FA-p** after 10h.

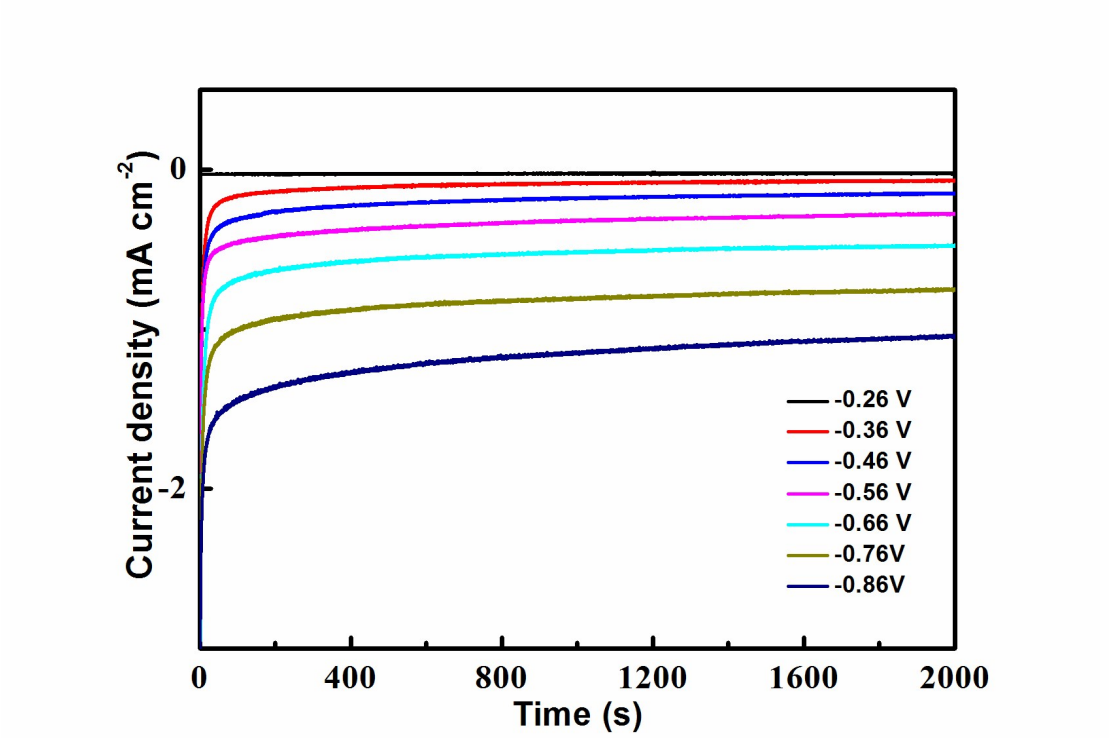

Fig. S9 Current density variation during electrochemical reduction of CO_2 in 0.1M $NaHCO_3$ aqueous solution by the **ZIF-FA-p** at various potentials (E_{VS} RHE).

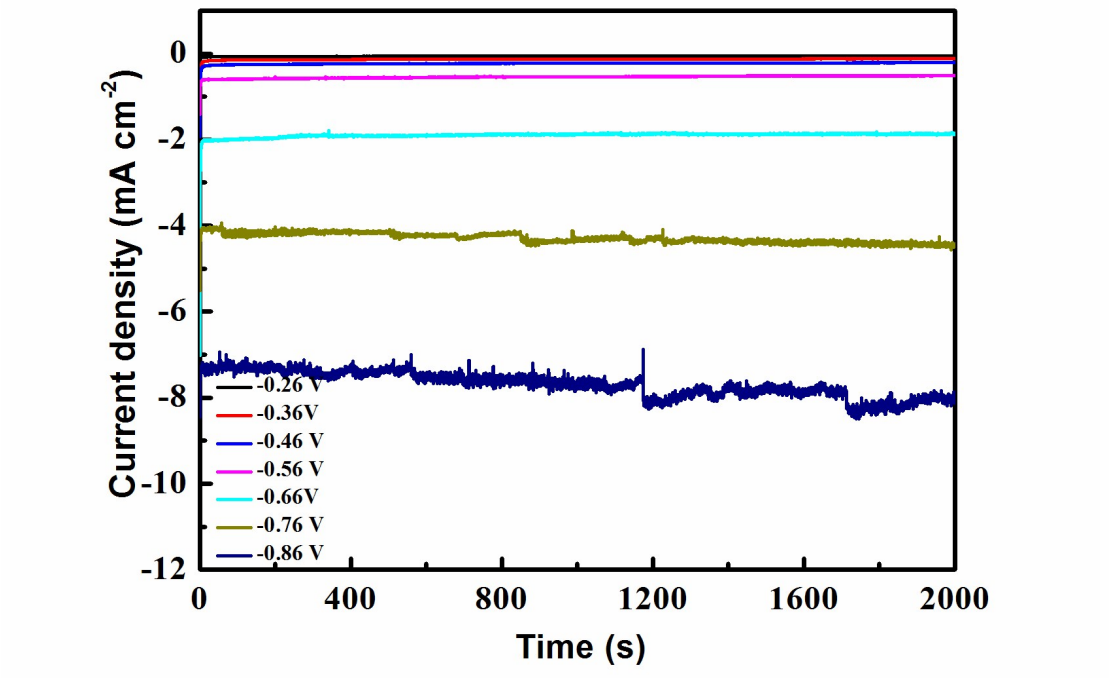

Fig. S10 Current density variation during electrochemical reduction of CO_2 in 0.1M $NaHCO_3$ aqueous solution by the **ZIF-CNT-FA-p** at various potentials (E_{VS} RHE).

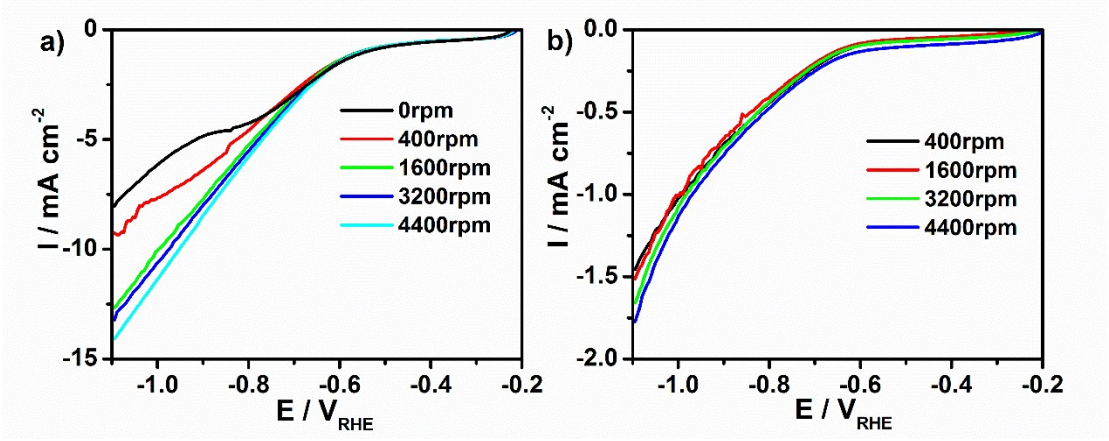

Fig. S11 Linear sweep voltammetry (LSV) of of **ZIF-CNT-FA-p** (a) and **ZIF-FA-p** (b) from -0.2 to -1.1 V_{RHE} in CO_2-saturated 0.1 M $NaHCO_3$ solution using a rotating disk electrode (RDE) at different rotating speeds.

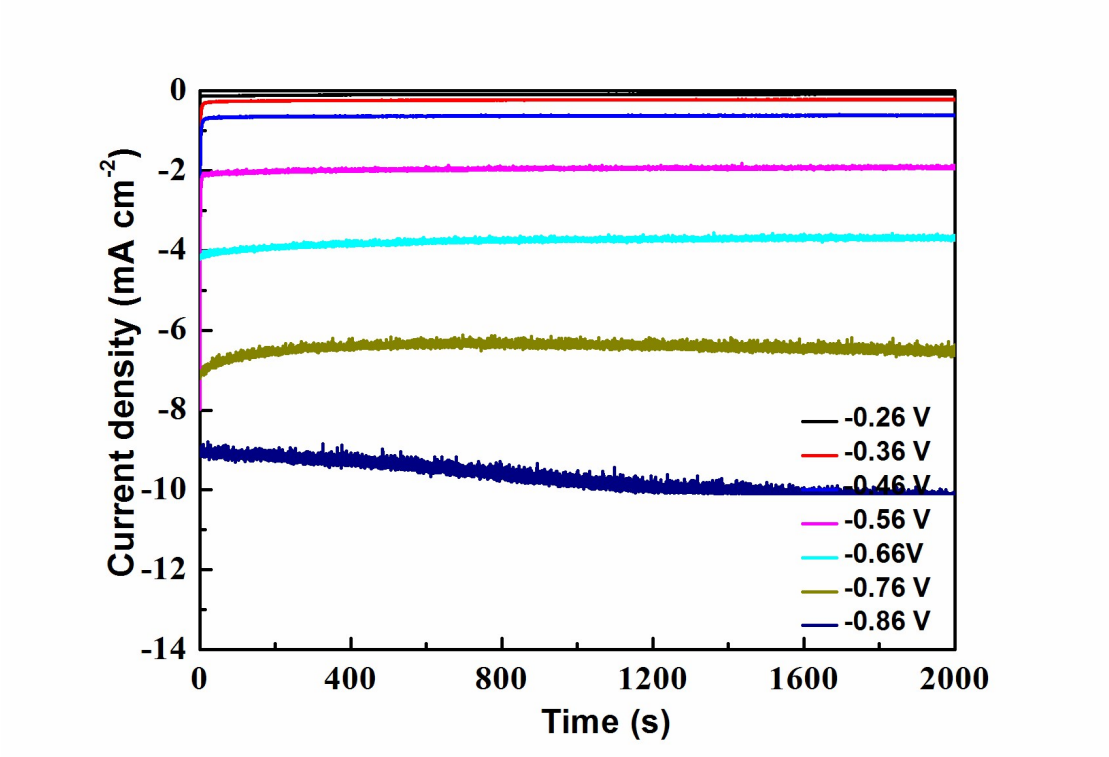

Fig. S12 Current density variation during electrochemical reduction of CO_2 in 0.1M $NaHCO_3$ aqueous solution by the **ZIF-Fe-CNT-FA-p** at various potentials (E_{VS} RHE).

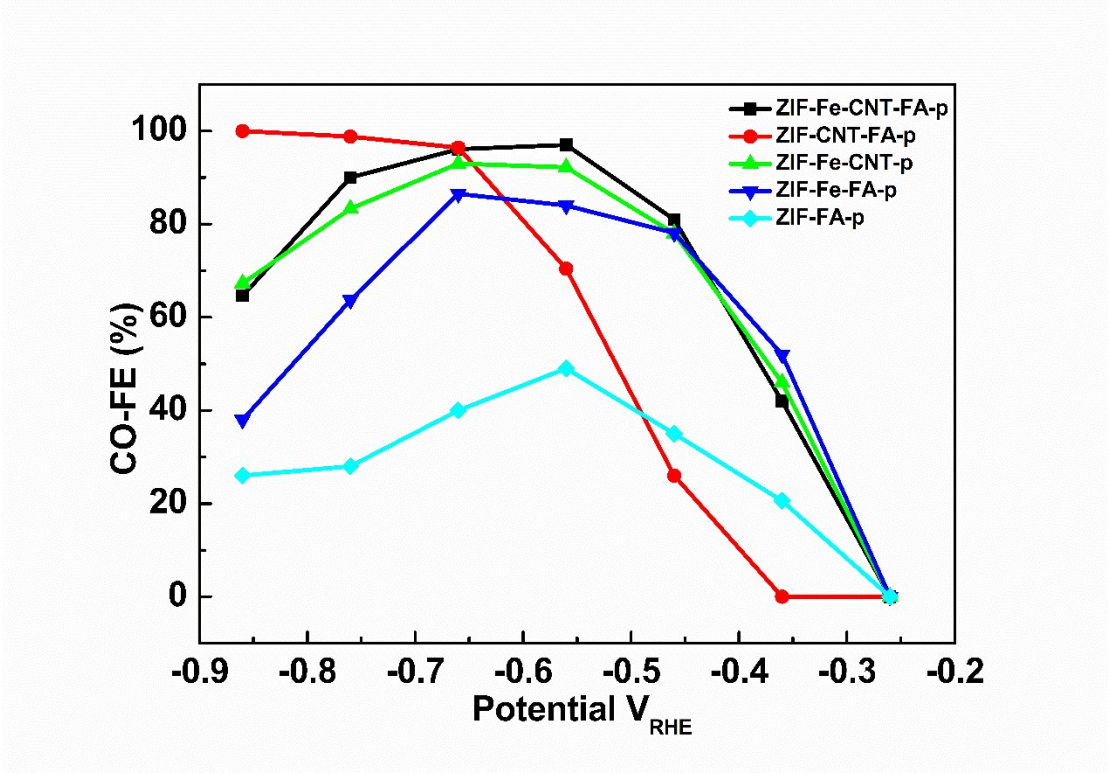

Fig. S13 Faradaic efficiency for CO versus potentials on different pyrolyzed ZIFs in CO_2 saturated 0.1M $NaHCO_3$.

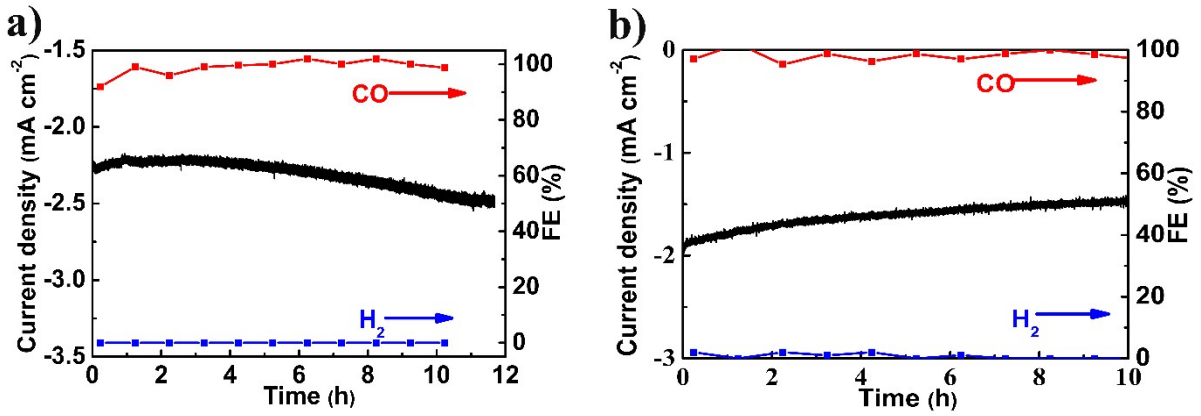

Fig. S14 Stability test of electrochemical CO_2 reduction by a) **ZIF-CNT-FA-p** at -0.66 V_{RHE} and b) **ZIF-Fe-CNT-FA-p** at -0.56 V_{RHE} during 10 h operation.

Table S1. BET surface areas and and specific capacitances of different samples.

Electrode	BET Surface area (m^2g^{-1})	Capacitance (F/g)
ZIF-CNT-FA-p	637.2	58.3
ZIF-Fe-CNT-FA-p	583.1	21.5
ZIF-FA-p	858.9	4.1

Table S2. Zn and Fe contents of different samples.

Sample	content wt %	
	Zn	Fe
ZIF-CNT-FA-p	0.1%	undetected
ZIF-Fe-CNT-FA-p	1.1%	2.7%
ZIF-FA-p	4.0%	undetected
ZIF-Fe-FA-p	4.2%	2.6%
MWCNT	0.01	undetected

Table S3. C and N contents of different samples

Sample	content wt %	
	C	N
ZIF-CNT-FA-p	76.60	5.56
ZIF-Fe-CNT-FA-p	71.33	5.71
ZIF-FA-p	64.07	9.51
ZIF-Fe-FA-p	73.29	9.63